Activation of p53 by Nutlin-3a, an antagonist of MDM2, induces apoptosis and cellular senescence in adult T-cell leukemia cells.

Hiroo Hasegawa,[1] Yasuaki Yamada,[1] Hidekatsu Iha,[2] Kunihiro Tsukasaki,[3] Kazuhiro Nagai,[4] Sunao Atogami,[1] Kazuyuki Sugahara,[1] Kazuto Tsuruda,[1] Akiko Ishizaki,[1] Shimeru Kamihira [1]

[1]Department of Laboratory Medicine and [3]Department of Hematology, Atomic Disease Institute, Nagasaki University Graduate School of Biomedical Sciences, Nagasaki, Japan

[2]Department of Infectious Diseases, Faculty of Medicine, Oita University, Yufu, Oita, Japan

[4]Transfusion Service, Nagasaki University Hospital of Medicine and Dentistry, Nagasaki, Japan

Corresponding author: Yasuaki Yamada, M.D., Ph.D.

Department of Laboratory Medicine, Nagasaki University Graduate School of

Biomedical Sciences, 1-7-1 Sakamoto, Nagasaki City, 852-8501, Japan

Tel.: +81-95-849-7408; Fax: +81-95-849-7422

E-mail: y-yamada@nagasaki-u.ac.jp

Running title: Nutlin-3a induces senescence in ATL cells.

Grant support note; This study was supported in part by a Grant-in-aid for Scientific Research (18590510) from the Japan Society for the Promotion of Science.

Abstract

It has been reported that the induction of cellular senescence through p53 activation is an effective strategy in tumor regression. Unfortunately however, tumors including adult T-cell leukemia/lymphoma (ATL) have disadvantages such as p53 mutations and a lack of $p16^{INK4a}$ and/or $p14^{ARF}$. In this study, we characterized Nutlin-3a-induced cell death in 16 leukemia/lymphoma cell lines. Eight cell lines, including 6 ATL-related cell lines, had wild-type p53, and Nutlin-3a activated p53 and the cell lines underwent apoptosis or cell-cycle arrest, while 8 cell lines with mutated p53 were resistant. Interestingly, SA-β-gal staining revealed that only ATL-related cell lines with wild-type p53 exhibited cellular senescence, although they lack both $p16^{INK4a}$ and $p14^{ARF}$. These results indicate that cellular senescence is an important event in p53-dependent cell death in ATL cells and is inducible without $p16^{INK4a}$ and $p14^{ARF}$. Furthermore, knockdown of TIGAR, a novel target gene of p53, by siRNA indicated its important role in the induction of cellular senescence. Since many patients with ATL carry wild-type p53, our study suggests that p53 activation by Nutlin-3a is a promising strategy in ATL. We also found synergism with a combination of Nutlin-3a and TRAIL, suggesting the application of Nutlin-3a-based therapy to be broader than expected.

Key words

p53, senescence, apoptosis, $p14^{ARF}$, Adult T-cell Leukemia, nutlin

Introduction

DNA damage activates the tumor-suppressor protein p53 as part of the surveillance mechanism.[1] Through the transcriptional activation or inactivation of target genes, p53 executes the appropriate physiological response, such as apoptosis, cell-cycle arrest, or senescence.[2] To date, a number of target genes involved in p53-induced apoptosis have been identified, such as *BAX*, *NOXA*, *PUMA*, *PIG3*, and *DR5*.[3,4] p53 can inhibit cell-cycle progression by initiating arrest at the G1, S, or G2 phase. An inhibitor of cyclin-dependent kinase $p21^{WAF1/CIP1}$ (p21), GADD45α, and 14-3-3σ have been implicated as major mediators of p53-induced growth arrest.[5] In addition, the recent discovery of a new target gene, C12orf5, also known as TP53-induced glycolysis, and an apoptosis regulator, TIGAR, revealed an unexpected function of p53 that regulates glucose metabolism and apoptosis.[6] Substantial evidence supports the idea that p53 can drive either apoptosis or cell-cycle arrest depending on which target genes it chooses to activate.[1,4] Meanwhile, a recent study showed that hematopoietic zinc finger (Hzf) is induced by p53 and binds to its DNA-binding domain, resulting in the preferential transactivation of pro-arrest p53 target genes over its pro-apoptotic target genes.[7,8] These findings suggest that Hzf acts as a key player in regulating cell fate decisions in response to genotoxic stress.

Cellular senescence is also an important mechanism in tumor suppression, which can be triggered by DNA damage or oncogene activation.[9] Cells entering cellular senescence are characterized by persistent cell-cycle arrest, a large flattened morphology, failure to replicate their DNA, and enzymatic activity senescence-associated-β-galactosidase (SA-β-gal). The tumor-suppressors $p16^{INK4a}$ (p16) and $p14^{ARF}$ (p14) have long been recognized as mediators of senescence, and research on oncogene-induced senescence has progressed rapidly; however, many questions remain regarding the programs and signals of cellular

senescence.[10,11]

Adult T-cell leukemia/lymphoma (ATL) is a neoplasm of T-lymphocyte origin etiologically associated with human T-cell lymphotropic virus type 1(HTLV-1), and is known to be resistant to standard anti-cancer therapies.[12-14] HTLV-1 Tax has been shown to interfere with most DNA repair mechanisms, prevent cell-cycle arrest and apoptosis, and contribute to the stepwise leukemic process leading to ATL.[15,16] Previous studies using a p53-responsive reporter plasmid pG13-Luc and/or γ-irradiation have demonstrated that Tax can repress the transcriptional activity of p53 in various transformed cell lines.[17-19] To date, several different mechanisms by which Tax inactivates p53 have been proposed, although the effects are indirect and complex.[20,21]

Mutations in the *p53* gene are found in about 50% of human cancers, and abrogate DNA binding or the transactivation of p53.[22] Wild-type p53 protein is inactivated through binding to a specific E3 ubiquitin ligase, MDM2, which mediates the degradation of p53. Recently, a small antagonist of MDM2, Nutlin-3a, has been developed. Nutlin-3a binds MDM2 in the p53-binding pocket, activates the p53 pathway in human cancer cells with wild-type p53, and has shown promising results in an animal tumor model.[23,24] Since mutated p53 proteins have been found in less than one-fourth of ATL cases and Tax expression is frequently lost in primary ATL cells, the activation of p53 by therapeutic drugs may become a promising approach to ATL therapy.[13,25]

Here we investigate the potential therapeutic utility of Nutlin-3a in a number of ATL-related cell lines. Our experiments also provide new insights into the mechanism of cellular senescence and possibility of expanding Nutlin-3a-based cancer therapy.

Materials and methods

Cell lines

ATL-derived cell lines ST1, KOB, LM-Y1, KK1, SO4, and OMT were established in our laboratory from the respective ATL patients.[26] These cell lines were maintained in RPMI 1640 medium supplemented with 10% FBS and 0.5U/ml of IL-2 (kindly provided by Takeda Pharmaceutical Company, Ltd., Osaka, Japan). We also used the ATL-derived cell line MT1, HTLV-1-infected T-cell lines MT2,[27] and HuT102,[28] human T cell leukemia cell lines Jurkat and MOLT-4, human B lymphoblastoid cell line SKW6.4, Burkitt lymphoma cell line Ramos, transformed follicular lymphoma cell line SUDHL-4, acute myeloid leukemia cell line HL-60, monocytic leukemia cell lines THP-1 and U937, and erythromyeloblastoid cell line K562. These cell lines were maintained in RPMI 1640 medium supplemented with 10% FBS.

Mutation analysis of p53

Total RNA from cell lines was isolated using ISOGEN (Wako, Osaka, Japan). After contaminating DNA was removed (Message Clean kit; GenHunter, Nashville, TN), cDNA was constructed using the Thermoscript RT-PCR System (Invitrogen, Carlsbad, CA) according to the manufacturer's protocol. RT-PCR was performed to amplify the sequence targeting the open reading frame of p53 (GenBank Accession number NM_000546) with the following primers: (forward); 5'-TCCGGGGACACTTTGCGTT-3', (reverse); 5'- AGGTGTGCGTCAGAAGCACC -3'. PCR products were then sequenced and analyzed using the BigDye Terminator v3.1 Cycle Sequencing kit (Applied Biosystems, Foster City, CA) and an ABI-PRISM model 310 Genetic Analyzer (Applied Biosystems). All mutations were confirmed by sequencing in both directions. Additional primers for sequencing were as follows: (forward); 5'-TGCATTCTGGGACAGCCAAGT-3', and 5'-CATCACACTGGAAGACTC-3',

(reverse); 5'- CCAAGTCTGTGACTTGCACGTACT-3', and 5'-GAGGAAGAGAATCTCCGCAAGAAAG-3'.

Deletion analysis of *p14* and *p16* and quantitative PCR for HTLV-I Tax

Since p16 and p14 share *exon 2* but have different open reading frames, loss of DNA in this region means the deletion of both proteins. Deletions of *p16* and *p14* were analyzed using *p16 exon 1 a* and *p14 exon 1ß,* respectively. We designed specific sets of primers and TaqMan probes as follows: for *p16 exon 1 a*: 5'-GAGCAGCATGGAGCCTTC-3' and 5'-CGTAACTATTCGGTGCGTTG-3', TaqMan probe: 6FAM-CCGCACCTCTACCCGACCC-TAMRA, for *p14 exon 1ß*: 5'-GCGCAGGTTCTTGGTGAC-3' and 5'-CCTGAGTAGCATCAGCACGA-3', TaqMan probe: 6FAM-TGTGAACCACGAAAACCCTCACTCG-TAMRA, for *INK4a/ARF exon 2*: 5'-ATTGAAAGAACCAGAGAGGC-3' and 5'-ACGTTAAAAGGCAGGACATT-3', TaqMan probe: 6FAM-ACCGAAGGTCCTACAGGGCCACAACT-TAMRA, and for *ß-globin*: 5'-CTTGAGGTTGTCCAGGTG-3' and 5'-TGCTGGTGGTCTACCCTT-3', TaqMan probe: 6FAM-GCCATGAGCCTTCACCTTAGGGTTG-TAMRA. Genomic DNA from cell lines was isolated using a QIAamp DNA Blood Mini Kit (Qiagen, Hilden, Germany) and subjected to a real-time quantitative PCR method based on TaqMan chemistry. PCRs were performed on a Roche LC480 (Roche Diagnostics, Basel, Switzerland) with LightCycler 480 Probes Master mix (Roche Diagnostics) according to the manufacturer's directions. All data were normalized to the *ß-globin* gene measured in the same samples. Samples with levels below the detection limit were considered to have homozygous deletions. Real-time quantitative PCR for HTLV-I Tax was performed as previously described.[29]

Chemicals and cell proliferation assay

Nutlin-3a (Alexis, San Diego, CA), recombinant human soluble-TRAIL (Biomol Research Laboratories, Plymouth Meeting, PA), and sodium butylate (Merck, Darmstadt, Germany) were used in this study. The cell proliferation assay (MTS assay) was performed with a Cell Titer 96® AQueos Cell Proliferation Assay kit (Promega, Madison, WI) in accordance with the manufacturer's instructions. Determination of the synergistic effect of combined treatment with Nutlin-3a and TRAIL was achieved with isobolographic analysis, as described previously.[30]

Flow cytometric detection of apoptosis, cell-cycle analysis, and death receptors

Apoptosis and the cell-cycle were examined by flow cytometry (FCM). To evaluate apoptotic changes, cells were stained simultaneously with Annexin-V and PI (Bender Medsystems, Vienna, Austria). Cell-cycle measurements based on DNA content were performed using a CycleTEST PLUS DNA reagent kit (BD Biosciences, San Jose, CA). Cells were harvested after treatment and analyzed using a FACSCalibur flowcytometer and Cellquest software (BD Biosciences). The cell-surface expression of death receptors was examined by FCM using DR5 (Alexis), or CD95 (BD Biosciences) monoclonal antibodies. Mouse IgG1 (DAKO, Kyoto, Japan) was used as a negative control.

Cellular senescence assay

For SA-ß-gal staining, cells were harvested after treatment, and then placed on glass slides by cytospin centrifugation at 700 g for 5 minutes. Fixation of cells and staining for SA-ß-gal in a humidified box at 37°C overnight at pH 6.0 were performed using the Senescent Cells Staining kit (Sigma Chemicals). The slides were washed 3 times in PBS and evaluated. May-Grünwald Giemsa staining was also performed to distinguish between nuclear material and the cytoplasm. Cells were considered positive when the cytoplasm was stained with SA-ß-gal.

Western-blot analysis and antibodies

Whole cell lysates (20–40μg) were prepared and Western blotting was performed as described previously.[31] Analysis was performed using antibodies to p53 (DO-1), MDM2 (Ab-1), PUMA, NOXA, and PIG3 (Merck), caspase-3, BAX, Bcl-xL, and p21 (Cell Signaling Technology, Beverly, MA), TIGAR and Hzf (Abcam, Cambridge, MA), GADD45α and p27 (Santa Cruz Biotechnology, Santa Cruz, CA), Bcl-2 and 14-3-3σ (Upstate Biotechnology, Waltham, MA), c-FLIP (Dave-2) (Alexis), survivin (R&D Systems Inc., Minneapolis, MN), DEC-1 (Novus Biologicals, Littleton, CO), DcR2 (Cayman Chemical, Ann Arbor, MI), and β-actin and α-tubulin (Sigma Chemicals, St Louis, MO). HTLV-1 Tax was detected by anti-Tax monoclonal antibodies from the NIH AIDS Research Reference Reagent Program.[32]

Luminex protein analysis

Protein expression of total p53 and phospho-p53^{ser15} was measured using a bead multiplex system (BioSource International, Camarillo, CA). Samples were incubated for 2 hours at room temperature with anti-p53 or anti-phospho-p53^{ser15} beads in a 96-well plate. Detector antibodies were added to each well and incubated for 1 hour, and the plate was read on a Luminex100 IS instrument (Luminex, Austin, TX). The concentrations of p53 and phospho-p53^{ser15} were determined from a standard curve assayed at the same time with known amounts of recombinant p53 and phospho-p53^{ser15}. This method permits quantitative analysis of p53 protein or phospho-p53^{ser15}, which is considered difficult in Western blot analysis.

p53-DNA Binding Enzyme-linked Immunosorbent Assay

The TransAM^{TM} p53 Transcription Factor Assay kit (Active Motif, Carlsbad, CA) was used following the manufacturer's protocol. Nuclear extracts from cells were prepared using a Nuclear/Cytosol Fractionation kit (BioVision, San Diego, CA) according to the manufacturer's protocol. Samples were diluted to 10 μg

total protein with lysis buffer and applied to plates containing an immobilized oligonucleotide containing the p53 consensus binding site. After one hour at room temperature, plates were washed and incubated with p53 antibody for another hour. After incubation with the secondary antibody, developing solution was added, incubation was continued to allow color development, and absorbance was read at 450 nm with a reference wavelength of 650 nm.

Transfection, Luciferase assay, and Small Interfering RNA

Transfection was performed with a Cell Line Nucleofector kit V or kit T and the Nucleofector™ system (Amaxa Biosystems, Cologne, Germany). The transfection program for ST1 (O-17), HuT102 (O-16), KOB (T-20), and KK1 cells (T-20) was determined so that high levels of transfection efficiency and cell viability could be achieved (data not shown). Cells were transfected with the luciferase reporter plasmid containing 13 copies of a p53 consensus binding site (pG13-Luc) and incubated with or without Nutlin-3a for 24 hours.[20] Luciferase activity in 10 μg cell lysate was measured using luciferase assay reagents (Promega) according to the manufacturer's instructions in a TD-20/20 luminometer (Turner Designs, Sunnyvale, CA). Each experiment was carried out in triplicate. Small interfering RNA (siRNA) of p21 (Silencer Validated siRNA #1621), TIGAR (Silencer Select siRNA #s32679), and control siRNA (Silencer negative control # 1) were purchased from Applied Biosystems. Each siRNA was transfected at a final concentration of 20nM. At 24 hours after transfection, cells were used for experimentation.

Results

Mutations of *p53* and deletions of *p14* and *p16*

We first analyzed the p53 status of 16 hematological cell lines, including 9 ATL-related cell lines, and

found that 8 had wild-type p53 and 8 had mutated p53 (Table-1). ST1, KOB, and OMT had single nucleotide polymorphisms (SNPs) at codon 72, which is the most extensively studied SNP in p53.[22] Consistent with previous reports, there was no mutation in p53 of HuT102, MT2, SUDHL-4, and MOLT-4 cells.[33-35] Mutations detected in Ramos and Jurkat, deletions in HL60, and an insertion in K562 cells were all in accord with previous reports [34,36-38] or the data from IARC (http://www-p53.iarc.fr/). Accordingly, 6 of 9 ATL-related cell lines carried wild-type p53 in our analysis. The results of deletion analysis of *p16* and *p14* genes are summarized in Table 1. Deletions of both *p16* and *p14* occurred in all ATL-derived cell lines, and 11 cell lines lacked both, irrespective of their p53 status.

Nutlin-3a induces cell-growth inhibition and accumulation of p53

We next examined the effect of Nutlin-3a on the growth of the 16 cell lines. All 8 cell lines with wild-type p53 showed apparent growth inhibition following treatment with Nutlin-3a, but the 8 cell lines with mutated p53 were resistant (Figure 1A and B). Since Nutlin-3a is expected to stabilize and activate p53 protein, we first examined the basal expression levels of p53-related proteins by Western blot analysis (Figure 1C). Among p53 wild-type cell lines, ATL-related cell lines had elevated basal levels of p53 and some cells also had detectable levels of p21 in agreement with previous reports.[33,39,40] Four p53-mutated cell lines showed strong expression of p53, probably due to mutations, and the others showed almost no band, consistent with the fact that they have deletions or nonsense mutations (Table 1). Importantly, these results were in accord with those of Luminex analysis (Figure 1D). Although KOB, LM-Y1, and K562 showed a faint expression of p27, other cell lines did not express detectable levels of p27. HTLV-1 Tax protein was detected in HuT102, MT2, OMT, and KOB, which is coincident with the results of mRNA expression (Table 1). In Luminex analysis, p53 wild-type cell lines showed a 4- to 12-fold increase in p53

expression after 24-hour exposure to Nutlin-3a as a result of the inhibition of p53 degradation, which was not observed in p53-mutated cell lines (Figure 1D). Furthermore, time-dependent accumulation of p53 and MDM2 was clearly detected by Western blot analysis (Figure 1E and not shown). Meanwhile, there was no change in the expression of HTLV-1 Tax by Nutlin-3a treatment (Figure 1E).

Activation of p53 by Nutlin-3a in ATL-related cell lines

In addition to the accumulation of p53 protein, we further evaluated transcriptional activities of p53 from various perspectives. We first investigated the level of DNA-binding activity of p53 by ELISA. When cells were treated with Nutlin-3a, all p53 wild-type cells showed higher activities than positive control cells (Figure 2A). Next, we transfected ST1, HuT102, KOB, and KK1 cells with a luciferase reporter plasmid, pG13-Luc, treated with or without Nutlin-3a, and performed a luciferase assay. As a result, fold inductions of luciferase activities were observed in a dose-dependent manner and showed maximum activities with 5μM Nutlin-3a in ST1 and HuT102 cells, while KK1 cells with mutated p53 showed no change (Figure 2B). Luminex analysis revealed that Nutlin-3a caused obvious phosphorylation of p53, a 4- to 20-fold increase, in all p53 wild-type cell lines, which had not occurred in KK1 cells (Figure 2C). These results indicate that Nutlin-3a causes the accumulation, increase of transcriptional activity, and phosphorylation of p53 in ATL-related cell lines with endogenous wild-type p53.

Nutlin-3a causes apoptosis in p53 wild-type cells

To clarify the details of Nutlin-3a-induced cell death, we performed Annexin-V/PI staining in p53 wild-type cell lines. We found weak apoptotic changes with 10μM Nutlin-3a and less than 30% of cells became positive for Annexin-V, except MOLT-4 cells, which showed apparent apoptosis (Figure 3A and 3B). In contrast, with more than 20μM Nutlin-3a, all p53 wild-type cell lines showed rapid apoptosis and

almost no living cell fraction was observed by Annexin-V/PI staining. These results suggest that Nutlin-3a eventually causes apoptosis in p53 wild-type cell lines in a dose-dependent manner. We then performed Western blot analysis of key molecules of the p53 pathway. In addition to cleaved forms of caspase-3, we found dose-dependent increase of BAX, PUMA, NOXA, and Hzf, no change of Bcl-2, and dose-dependent decrease of XIAP and survivin (Figure 3C).

Nutlin-3a induces cellular senescence followed by cell-cycle arrest in p53 wild-type cells

Despite weak apoptotic changes, cell growth of p53 wild-type cell lines was significantly depressed by Nutlin-3a at a concentration of 10μM. To clarify this discordance, we performed cell cycle analysis. When cells were treated with 10μM Nutlin-3a for 24 hours, these cells showed significant cell-cycle arrest in the G1 phase instead of apoptosis. The G1 cell population increased from 63% to 78% in ST1 and from 68% to 92% in HuT102 (Figure 4A). Similar results were observed in the other p53 wild-type cell lines (Figure 4B). Although it has been reported that p53 plays a central role in the induction of cellular senescence, Nutlin-3a-induced cellular senescence has not been reported in leukemia cells.[41,42] We thus performed SA-ß-gal staining as a marker of cellular senescence after incubation with 10μM Nutlin-3a for 72 hours. Five of 8 p53 wild-type cell lines (ST1, HuT102, MT2, OMT, and KOB) were clearly stained by SA-ß-gal and all were ATL-related cell lines (Figure 4C and not shown). No non-ATL cell lines became positive for SA-ß-gal staining. In contrast, after treatment with 1mM sodium butylate, a well-known senescence inducer, all cell lines examined, including those with mutant p53 (SO4 and K562), became positive for SA-β-gal staining (data not shown). Among 5 SA-ß-gal-positive cell lines, 3 lacked both p16 and p14 (Table 1), suggesting that these cells underwent p53-dependent cellular senescence without the participation of p16 and/or p14. We further investigated whether removal of Nutlin-3a alters cell fate;

senescence or cell proliferation. To this purpose, p53 wild-type ATL cell lines were cultured with Nutlin-3a for 72 hours to induce cellular senescence. Then, cells were harvested, washed, and incubated with or without Nutlin-3a for another 48 hours. Nulin-3a re-treated cells as well as washed-out cells continuously showed G1 cell-cycle arrest and were persistently positive for SA-ß-gal staining (Figure 4D and not shown). In addition, cell proliferation assay revealed that "senescent" cells were not proliferated even after wash-out of Nutlin-3a (Figure 4E). These results indicate that Nutlin-3a-induced cellular senescence, as a result of continuous growth arrest, is irreversible change.

Analysis of molecules involved in p53-dependent cellular senescence

Little is known about the key molecules or markers of cellular senescence. To explore such molecules, we performed Western blot analysis comparing the cellular senescence setting with the apoptotic setting (Figures 5A and 3C). As expected, p21 expressions increased in the senescence setting (Figure 5A) but rather decreased in the rapid apoptotic setting (Figure 3C). Most of the typical effectors of apoptosis, BAX, PUMA, and NOXA, tended to increase and anti-apoptotic factors, such as XIAP and survivin, decreased even when cells were induced to cell-cycle arrest and senescence (Figure 5A). The expressions of p27, 14-3-3σ, and $FLIP_L$ were increased in ST1 cells but not in HuT102 cells (Figure 5A). Of note, PIG3 and TIGAR were increased in a time-dependent manner in both ST1 and HuT102 cells (Figure 5A), which was not observed in the apoptotic setting (Figure 3B). Collectively, these results suggest that the activations of p21, PIG3, and TIGAR are important in the induction of cellular senescence. Although we expected that Hzf would play a key role in determining either progression to cell-cycle arrest with senescence or apoptosis, we did not find any significant differences between the two settings.

Novel evidence that TIGAR plays a role in cellular senescence

Previous studies reported that PIG3 plays a critical role in p53-dependent apoptosis and that p21 can contribute to cellular senescence as well as cell-cycle arrest.[2,4] We first performed a knockdown experiment of p21 with siRNA in ST1 cells. When control-siRNA cells and p21-siRNA cells were treated with Nutlin-3a, 56% reduction of SA-ß-gal-positive cells was observed in p21-siRNA cells compared to control-siRNA cells (data not shown). Next, we focused on TIGAR and performed siRNA experiments using ST1 and HuT102 cells because the study of TIGAR started only recently and its role in p53-depedent cell death remains unclear.[6] We confirmed that control-siRNA cells showed up-regulated TIGAR expression after Nutlin-3a treatment, which was effectively suppressed by TIGAR-siRNA (Figure 5B). Although TIGAR is reported to be an inhibitor of apoptosis, siTIGAR did not enhance apoptosis but rather reduced Annexin-V-positive cells (Figure 5C). In a cellular senescence setting, the proportion of SA-ß-gal-positive cells was significantly reduced in TIGAR-siRNA cells (reduced to 48% and 29% in ST1 cells and HuT102 cells, respectively) (Figure 5D). Similar results were also obtained in KOB cells (data not shown). These results suggest that TIGAR plays an important role in the induction of cellular senescence.

Synergistic effect of Nutlin-3a and TRAIL

Since some death receptors (DRs) are known as downstream genes of p53, we investigated the cell-surface expression of DRs by FCM.[4] As a result, most p53 wild-type cell lines showed the up-regulation of Fas (DR for Fas-ligand) and DR5 (DR for TRAIL) expressions after Nutlin-3a treatment (Figure 6A). Our previous studies showed that although ATL cells are resistant to TRAIL, up-regulation of DR5 expression can overcome TRAIL resistance.[26,43] In fact, ST1 and KOB cells were resistant to TRAIL and the IC_{50} of each cell line was very high, 13.5 and 17.1μg/ml, respectively. Of note, the combination of Nutlin-3a and

TRAIL significantly decreased cell proliferation and synergistic effects were confirmed by isobolographic analysis (Figure 6B). As shown in Figure 6C, although the IC_{50} of ST1 and KOB cells for Nutlin-3a was 6.85 and 11.35 μM, respectively, a combination of 2.5μM Nutlin-3a and only 0.6μg/ml TRAIL markedly increased the proportion of Annexin-V-positive cells compared to cells treated with either agent alone (from 32.0% and 21.2% to 82% in ST1 cells and from 9.0% and 19.3% to 52% in KOB cells). These results indicate that, with the combined use of TRAIL, the dose of Nutlin-3a could be successfully reduced.

Discussion

Cellular senescence is emerging as an important *in vivo* anticancer response elicited by multiple stresses. Recent reports have shown that cancers in mice can be eliminated through the activation of a single gene *p53* and that cellular senescence is a primary mechanism of tumor regression.[44-46] Nutlin-3a was reported to induce apoptosis in various cancer cells with functional p53; however, the induction of cellular senescence in leukemia cells has not been reported.[41,42,47,48] In this study, we showed for the first time that Nutlin-3a induces cellular senescence in a number of ATL-related cell lines with wild-type p53.

Although the relative importance of *p16*, *p14*, and *p53* in cellular senescence is still unclear and the mechanism is thought to be different in humans versus mice or by cell type, there is evidence to suggest that p14ARF is closely associated with the induction of cellular senescence in mice.[10,11,49] Consistent with this scenario, cells without both *p16* and *p14* have not been shown to undergo cellular senescence, as far as we know. In this study however, although most ATL-related cell lines examined lacked both *p16* and *p14*, Nutlin-3a did induce cellular senescence in these cells, suggesting that p53-dependent cellular senescence was induced without the participation of *p16* and *p14*. Markers of cellular senescence may be useful as

diagnostic or prognostic tools and may help to monitor treatment response. In addition to SA-ß-gal, *p16*, and *p14*, Collado *et al*. identified *de novo* markers of cellular senescence using oncogene-induced senescent cells.[50] These markers were $p15^{INK4b}$, BHLHB2 (Dec1), and TNFRSF10D (DcR2). In this study, we did not find any change in the level of protein expression of Dec1 and DcR2 in cells which underwent cellular senescence. Instead, we found apparent up-regulation of p27, 14-3-3σ and $FLIP_L$ in ST1 cells and these changes were not observed in apoptotic cells. More importantly, the expression of TIGAR was increased in both ST1 and HuT102 cells during cellular senescence. In addition, using TIGAR-siRNA, we demonstrated that TIGAR plays an important role in the induction of cellular senescence. Our results suggest that TIGAR is a novel maker of cellular senescence. In this aspect, Bensaad *et al*. proposed that TIGAR might modulate the apoptotic response, allowing cells to survive following stress signals.[6] Since the inhibition of apoptosis is one of the important processes of cellular senescence, knockdown of TIGAR may result in the inhibition of cellular senescence. Another important point is that all cells which underwent senescence were ATL-related cell lines. ATL cells are known to be resistant to various apoptotic signals, the mechanism of which may lead ATL cells towards cellular senescence. A previous report pointed out that an antiviral drug, Zidovudine (AZT), can activate p53 in ATL cells and that cellular senescence contributes to AZT-induced cell death.[51] Supporting their theory, our study clearly indicated that cellular senescence is an important pathway of p53-dependent cell death in ATL cells.

Although it has been thought that the p53 pathway is disturbed in ATL cells by HTLV-1 Tax,[15,21] other chemicals alternatively activate p53 through inhibition of the NFκB or PI3K/AKT pathway and induce apparent cell-cycle arrest and/or apoptosis.[52-54] In our study, Nutlin-3a caused rapid apoptosis in a number of ATL-related cell lines with wild-type p53, and typical targets of p53, such as BAX, NOXA, PUMA, DR5,

and survivin, actually responded to Nutlin-3a treatment. These results indicate that Nutlin-3a can overcome Tax-induced p53 impairment even in cells with high Tax expression. Meanwhile, a recent report showed that Tax binds the anaphase promoting complex (APC), stabilizes the expression of p21 and p27 independently of p53, and induces rapid senescence.[55] It was suggested that evading senescence through a loss of p27 is critical for cell transformation and the development of ATL. This scenario, an early event in the development of ATL, might not be reflected by the ATL-related cell lines used in this study; however, up-regulation of p27 in ST1 cells when they underwent senescence is quite suggestive.

Previous studies have demonstrated that the use of Nutlin-3a in combination with genotoxic drugs is more effective in leukemia cells than each agent alone.[41,42] On the other hand, a recent report pointed out that rapid MDM2 reduction or profound p53 activation in mice results in an unfavorable outcome.[56] In our study, TRAIL successfully reduced the dose of Nutlin-3a and showed synergism. TRAIL-related drugs (soluble-TRAIL or antibodies to DR4 or DR5) are now in clinical trials and combination therapy with other anti-neoplastic agents is now becoming important.[57,58] Since p53-induced pro-apoptotic molecules, including DR5, were up-regulated and anti-apoptotic molecules were decreased by Nutlin-3a treatment, the combinatory use of TRAIL-related drugs may be one of the most rational choices for Nutlin-3a-based cancer therapy.

Acknowledgements; We are grateful to Dr Norman E. Sharpless, Departments of Medicine and Genetics, The Lineberger Comprehensive Cancer Center, The University of North Carolina, for his critical review and constructive suggestions on this manuscript.

References

1 Horn HF, Vousden KH. Coping with stress: multiple ways to activate p53. *Oncogene* 2007; **26**: 1306-1316.

2 Helton ES, Chen X. p53 modulation of the DNA damage response. *J Cell Biochem*. 2007; **100**: 883-896.

3 Chipuk JE, Green DR. Dissecting p53-dependent apoptosis. *Cell Death Differ* 2006; **13**: 994-1002.

4 Levine AJ, Hu W, Feng Z. The P53 pathway: what questions remain to be explored? *Cell Death Differ* 2006; **13**: 1027-1036.

5 Yu J, Zhang L. The transcriptional targets of p53 in apoptosis control. *Biochem Biophys Res Commun* 2005; **331**: 851-858.

6 Bensaad K, Tsuruta A, Selak MA, Vidal MN, Nakano K, Bartrons R et al. TIGAR, a p53-inducible regulator of glycolysis and apoptosis. *Cell* 2006; **126**: 107-120.

7 Sugimoto M, Gromley A, Sherr CJ. Hzf, a p53-responsive gene, regulates maintenance of the G2 phase checkpoint induced by DNA damage. *Mol Cell Biol* 2006; **26**: 502-512.

8 Das S, Raj L, Zhao B, Kimura Y, Bernstein A, Aaronson SA et al. Hzf Determines cell survival upon genotoxic stress by modulating p53 transactivation. *Cell* 2007; **130**: 624-637.

9 Collado M, Blasco MA, Serrano M. Cellular senescence in cancer and aging. *Cell* 2007; **130**: 223-233.

10 Kim WY, Sharpless NE. The regulation of INK4/ARF in cancer and aging. *Cell* 2006; **127**: 265-275.

11 Satyanarayana A, Rudolph KL. p16 and ARF: activation of teenage proteins in old age. *J Clin Invest* 2004; **114**: 1237-1240.

12 Yoshida M Discovery of HTLV-1, the first human retrovirus, its unique regulatory mechanisms, and insights into pathogenesis. *Oncogene* 2005; **24**: 5931-5937.

13 Taylor GP, Matsuoka M. Natural history of adult T-cell leukemia/lymphoma and approaches to therapy. *Oncogene* 2005; **24**: 6047-6057.

14 Yamada Y, Tomonaga M. The current status of therapy for adult T-cell leukaemia-lymphoma in Japan. *Leuk Lymphoma* 2003; **44**: 611-618.

15 Grassmann R, Aboud M, Jeang KT. Molecular mechanisms of cellular transformation by HTLV-1 Tax. *Oncogene* 2005; **24**: 5976-5985.

16 Marriott SJ, Semmes OJ. Impact of HTLV-I Tax on cell cycle progression and the cellular DNA damage repair response. *Oncogene* 2005; **24**: 5986-5995.

17 Akagi T, Ono H, Tsuchida N, Shimotohno K. Aberrant expression and function of p53 in T-cells immortalized by HTLV-I Tax1. *FEBS Lett* 1997; **406**: 263-266.

18 Pise-Masison CA, Choi KS, Radonovich M, Dittmer J, Kim SJ, Brady JN. Inhibition of p53 transactivation function by the human T-cell lymphotropic virus type 1 Tax protein. *J Virol* 1998; **72**: 1165-1170.

19 Mulloy JC, Kislyakova T, Cereseto A, Casareto L, LoMonico A, Fullen J et al. Human T-cell lymphotropic/leukemia virus type 1 Tax abrogates p53-induced cell cycle

arrest and apoptosis through its CREB/ATF functional domain. *J Virol* 1998; **72**: 8852-8860.

20 Miyazato A, Sheleg S, Iha H, Li Y, Jeang KT. Evidence for NF-kappaB- and CBP-independent repression of p53's transcriptional activity by human T-cell leukemia virus type 1 Tax in mouse embryo and primary human fibroblasts. *J Virol* 2005; **79**: 9346-9350.

21 Pise-Masison CA, Jeong SJ, Brady JN. Human T cell leukemia virus type 1: the role of Tax in leukemogenesis. *Arch Immunol Ther Exp* (Warsz) 2005; **53**: 283-296.

22 Soussi T, Wiman KG. Shaping genetic alterations in human cancer: the p53 mutation paradigm. *Cancer Cell* 2007; **12**: 303-312.

23 Vassilev LT, Vu BT, Graves B, Carvajal D, Podlaski F, Filipovic Z et al. In vivo activation of the p53 pathway by small-molecule antagonists of MDM2. *Science* 2004; **303**: 844-848.

24 Vassilev LT. MDM2 inhibitors for cancer therapy. *Trends Mol Med* 2007; **13**: 23-31.

25 Tawara M, Hogerzeil SJ, Yamada Y, Takasaki Y, Soda H, Hasegawa H et al. Impact of p53 aberration on the progression of Adult T-cell Leukemia/Lymphoma. *Cancer Lett* 2006; **234:** 249-255.

26 Hasegawa H, Yamada Y, Harasawa H, Tsuji T, Murata K, Sugahara K et al. Sensitivity of adult T-cell leukaemia lymphoma cells to tumour necrosis factor-related apoptosis-inducing ligand. *Br J Haematol* 2005; **128**: 253-265.

27 Yoshida M, Miyoshi I, Hinuma Y. Isolation and characterization of retrovirus from

cell lines of human adult T-cell leukemia and its implication in the disease. *Proc Natl Acad Sci U S A* 1982; **79**: 2031-2035.

28 Posner LE, Robert-Guroff M, Kalyanaraman VS, Poiesz BJ, Ruscetti FW, Fossieck B et al. Natural antibodies to the human T cell lymphoma virus in patients with cutaneous T cell lymphomas. *J Exp Med*. 1981; **154:** 333-346.

29 Usui T, Yanagihara K, Tsukasaki K, Murata K, Hasegawa H, Yamada Y et al. Characteristic expression of HTLV-1 basic zipper factor (HBZ) transcripts in HTLV-1 provirus-positive cells. *Retrovirology* 2008; **5**: 34.

30 Berenbaum MC. A method for testing for synergy with any number of agents. *J Infect Dis* 1978; **137:** 122-130.

31 Hasegawa H, Yamada Y, Komiyama K, Hayashi M, Ishibashi M, Sunazuka T et al. A novel natural compound, a cycloanthranilylproline derivative (Fuligocandin B), sensitizes leukemia cells to apoptosis induced by tumor necrosis factor related apoptosis-inducing ligand (TRAIL) through 15-deoxy-Delta 12, 14 prostaglandin J2 production. *blood* 2007; **110**: 1664-1674.

32 Iha H, Kibler KV, Yedavalli VR, Peloponese JM, Haller K, Miyazato A et al. Segregation of NF-kappaB activation through NEMO/IKKgamma by Tax and TNFalpha: implications for stimulus-specific interruption of oncogenic signaling. *Oncogene*. 2003; **22:** 8912-23.

33 Reid RL, Lindholm PF, Mireskandari A, Dittmer J, Brady JN. Stabilization of wild-type p53 in human T-lymphocytes transformed by HTLV-I. *Oncogene* 1993; **8**:

3029-3036.

34 Cheng J, Haas M. Frequent mutations in the p53 tumor suppressor gene in human leukemia T-cell lines. *Mol Cell Biol* 1990; **10**: 5502-5509.

35 Sugito S, Yamato K, Sameshima Y, Yokota J, Yano S, Miyoshi I. Adult T-cell leukemia: structures and expression of the p53 gene. *Int J Cancer* 1991; **49**: 880-885.

36 Gaidano G, Ballerini P, Gong JZ, Inghirami G, Neri A, Newcomb EW et al. p53 mutations in human lymphoid malignancies: association with Burkitt lymphoma and chronic lymphocytic leukemia. *Proc Natl Acad Sci U S A* 1991; **88**: 5413-5417.

37 Sugimoto K, Toyoshima H, Sakai R, Miyagawa K, Hagiwara K, Ishikawa F et al. Frequent mutations in the p53 gene in human myeloid leukemia cell lines. *blood* 1992; **79**: 2378-2383.

38 Neubauer A, He M, Schmidt CA, Huhn D, Liu ET. Genetic alterations in the p53 gene in the blast crisis of chronic myelogenous leukemia: analysis by polymerase chain reaction based techniques. *Leukemia* 1993; **7**: 593-600.

39 Takemoto S, Trovato R, Cereseto A, Nicot C, Kislyakova T, Casareto L et al. p53 stabilization and functional impairment in the absence of genetic mutation or the alteration of the p14(ARF)-MDM2 loop in ex vivo and cultured adult T-cell leukemia/lymphoma cells. *blood* 2000; **95**: 3939-3944.

40 Cereseto A, Diella F, Mulloy JC, Cara A, Michieli P, Grassmann R et al. p53 functional impairment and high p21waf1/cip1 expression in human T-cell lymphotropic/leukemia virus type I-transformed T cells. *blood* 1996; **88**: 1551-1560.

41 Kojima K, Konopleva M, Samudio IJ, Shikami M, Cabreira-Hansen M, McQueen T et al. MDM2 antagonists induce p53-dependent apoptosis in AML: implications for leukemia therapy. *blood*. 2005; **106**: 3150-3159.

42 Coll-Mulet L, Iglesias-Serret D, Santidrián AF, Cosialls AM, de Frias M, Castaño E et al. MDM2 antagonists activate p53 and synergize with genotoxic drugs in B-cell chronic lymphocytic leukemia cells. *blood* 2006; **107**: 4109-4114.

43 Hasegawa H, Yamada Y, Komiyama K, Hayashi M, Ishibashi M, Yoshida T et al. Dihydroflavonol BB-1, an extract of natural plant Blumea balsamifera, abrogates TRAIL resistance in leukemia cells. *blood* 2006; **107:** 679-688.

44 Martins CP, Brown-Swigart L, Evan GI. Modeling the therapeutic efficacy of p53 restoration in tumors. *Cell* 2006; **127**: 1323-1334.

45 Xue W, Zender L, Miething C, Dickins RA, Hernando E, Krizhanovsky V et al. Senescence and tumour clearance is triggered by p53 restoration in murine liver carcinomas. *Nature* 2007; **445:** 656-660.

46 Ventura A, Kirsch DG, McLaughlin ME, Tuveson DA, Grimm J, Lintault L et al. Restoration of p53 function leads to tumour regression in vivo. *Nature* 2007; **445**: 661-665.

47 Tovar C, Rosinski J, Filipovic Z, Higgins B, Kolinsky K, Hilton H et al. Small-molecule MDM2 antagonists reveal aberrant p53 signaling in cancer: implications for therapy. *Proc Natl Acad Sci U S A* 2006; **103**: 1888-1893.

48 Van Maerken T, Speleman F, Vermeulen J, Lambertz I, De Clercq S, De Smet E et al.

Small-molecule MDM2 antagonists as a new therapy concept for neuroblastoma. *Cancer Res* 2006; **66**: 9646-9655.

49 Sherr CJ. Divorcing ARF and p53: an unsettled case. *Nat Rev Cancer* 2006; **6:** 663-673.

50 Collado M, Gil J, Efeyan A, Guerra C, Schuhmacher AJ, Barradas M et al. Tumour biology: senescence in premalignant tumours. *Nature* 2005; **436:** 642.

51 Datta A, Bellon M, Sinha-Datta U, Bazarbachi A, Lepelletier Y, Canioni D et al. Persistent inhibition of telomerase reprograms adult T-cell leukemia to p53-dependent senescence. *blood* 2006; **108**: 1021-9.

52 Dasgupta A, Jung KJ, Jeong SJ, Brady JN. Inhibition of methyltransferases results in induction of G2/M checkpoint and programmed cell death in human T-lymphotropic virus type 1-transformed cells. *J Virol* 2008; **82**: 49-59.

52 Jeong SJ, Dasgupta A, Jung KJ, Um JH, Burke A, Park HU et al. PI3K/AKT inhibition induces caspase-dependent apoptosis in HTLV-1-transformed cells. *Virology* 2008; **370**: 264-272.

54 Jung KJ, Dasgupta A, Huang K, Jeong SJ, Pise-Masison C, Gurova KV et al. Small-molecule inhibitor which reactivates p53 in human T-cell leukemia virus type 1-transformed cells. *J Virol* 2008; **82**: 8537-8547.

55 Kuo YL, Giam CZ. Activation of the anaphase promoting complex by HTLV-1 tax leads to senescence. *EMBO J* 2006; **25**: 1741-1752.

56 Ringshausen I, O'Shea CC, Finch AJ, Swigart LB, Evan GI. Mdm2 is critically and

continuously required to suppress lethal p53 activity in vivo. *Cancer Cell* 2006; **10**: 501-514.

57 Duiker EW, Mom CH, de Jong S, Willemse PH, Gietema JA, van der Zee AG et al. The clinical trail of TRAIL. *Eur J Cancer* 2006; **42**: 2233-2240.

58 Schaefer U, Voloshanenko O, Willen D, Walczak H. TRAIL: a multifunctional cytokine. *Front Biosci* 2007; **12**: 3813-3824.

Figure Legends

Figure 1. Sensitivity of hematological cell lines to Nutlin-3a and accumulation of p53 protein. (A and B) Cells ($5–7\times10^5$ /ml) were cultured for 48 hours with the indicated concentrations of Nutlin-3a, and cell proliferation (% against control cells) was evaluated by MTS assay. All experiments were performed in triplicate and the results are expressed as the mean ± SD. (C) Whole cell lysate (40μg) was prepared and basal expression levels of p53-related proteins were detected by Western blot analysis. (D and E) Cells were cultured with or without 10μM Nutlin-3a for 24 hours or the indicated period. (D) 10μg cell lysate was prepared and Luminex analysis was performed to evaluate the accumulation of p53 protein. Experiments were performed in duplicate and the results are expressed as the mean ± SD. (E) Whole cell lysate (20μg) was prepared and expression levels of p53-related proteins were detected by Western blot analysis. .

Figure 2. Transcriptional activation of p53 by Nutlin-3a treatment. Cells were treated with or without the indicated concentrations of Nutlin-3a for 24 hours. After cells were harvested, ELISA, luciferase assay, and Luminex analysis were performed. KK1 (p53 mutant) cells were used as an accumulation-negative control. (A) Nuclear extract from H_2O_2-treated MCF-7 cells contained in the kit was used as a positive control. 10μg nuclear extract was used, experiments were performed in duplicate, and results are expressed as the mean ± SD. (B) For the luciferase assay, cells were cotransfected with 0.1 μg pG13-Luc, incubated for 12 hours, and treated with or without Nutlin-3a for 24 hours. Experiments were performed in triplicate and results are expressed as the mean ± SD. The level of activation (fold induction) was obtained by setting the value without Nutlin-3a as 1.0. (C) 10μg whole cell lysate was prepared, experiments were performed in duplicate, and results are expressed as the mean ± SD. Fold induction was also obtained by setting the

value without Nutlin-3a as 1.0 and is indicated on the graph.

Figure 3. Analysis of molecules in Nutlin-3a-induced apoptosis. Cells were treated with or without the indicated concentrations of Nutlin-3a for 24 hours. After cells were harvested, flow cytometric analysis by Annexin-V/PI staining (A and B) and Western blot analysis (C) were performed.

Figure 4. Nutlin-3a induces cellular senescence followed by cell-cycle arrest. (A and B) Cells were treated with or without the indicated concentrations of Nutlin-3a for 24 hours. After cells were harvested, cell-cycle analysis was performed by FCM. (C) Similarly, after 72 hours, cells were harvested and SA-β-gal staining was performed and examined microscopically. Bar: 20μm. (D and E) Wash-out experiments. p53 wild-type cell lines were cultured with Nutlin-3a for 72 hours to induce cellular senescence. Then, cells were washed and incubated with or without Nutlin-3a for another 48 hours. SA-ß-gal staining (D) and MTS assay were performed (E).

Figure 5. Analysis of molecules in Nutlin-3a-induced cellular senescence. (A) Cells were treated with 10μM Nutlin-3a for the indicated period and Western-blot analysis was performed using the same antibodies as in Figure 3C. (B) Effects of TIGAR-siRNA. Twenty-four hours after transfection, cells were incubated for 24 hours with or without 10μM Nutlin-3a and Western blot analysis were performed. (C) Twenty-four hours after transfection, cells were incubated for 24 hours with or without 20μM Nutlin-3a, and Annexin-V/PI staining was performed by FCM. Experiments were performed in triplicate, Annexin-V-positive cells were counted, and results are expressed as the mean ± SD. (D) Twenty-four hours after transfection, cells were incubated for 72 hours with or without 5–10μM Nutlin-3a and SA-β-gal staining was performed. SA-β-gal-positive cells among 500 cells were counted both in si-control cells and si-TIGAR cells and the percentage against si-control cells was calculated. Results are expressed as the

mean ± SD of three independent studies and were also analyzed using Student's t-test.

Figure 6. Combination of Nutlin-3a and TRAIL induced synergistic effects. (A) Cells were treated with or without the indicated concentrations of Nutlin-3a. Cell-surface expression of death receptors was examined by FCM and evaluated by RFI (ratio of mean fluorescence intensity for specific staining to that for control staining) and the results are expressed as the mean ± SD. (B) ST1 and KOB cells were treated with the indicated concentration of Nutlin-3a for 24 hours, TRAIL was then added at the indicated concentration, and cell proliferation (% against control cells) was evaluated after another 24 hours by MTS assay. All experiments were performed in triplicate and the results are expressed as the mean ± SD. In isobolographic analysis, fractional inhibitory concentrations were determined using the IC_{50} of either agent alone or in combination. Sums of less than 1, 1, and greater than 1 indicate synergy, additivity, and antagonism, respectively. Four experimental points were found to be significantly below the theoretical additive line (dotted line), indicating a synergistic effect. (C) Combination of 2.5μM Nutlin-3a and 0.6μg/ml TRAIL. Annexin-V/PI staining was performed and percentages of intact cells and early and late apoptotic cells are indicated in the lower panels.

Figure 1

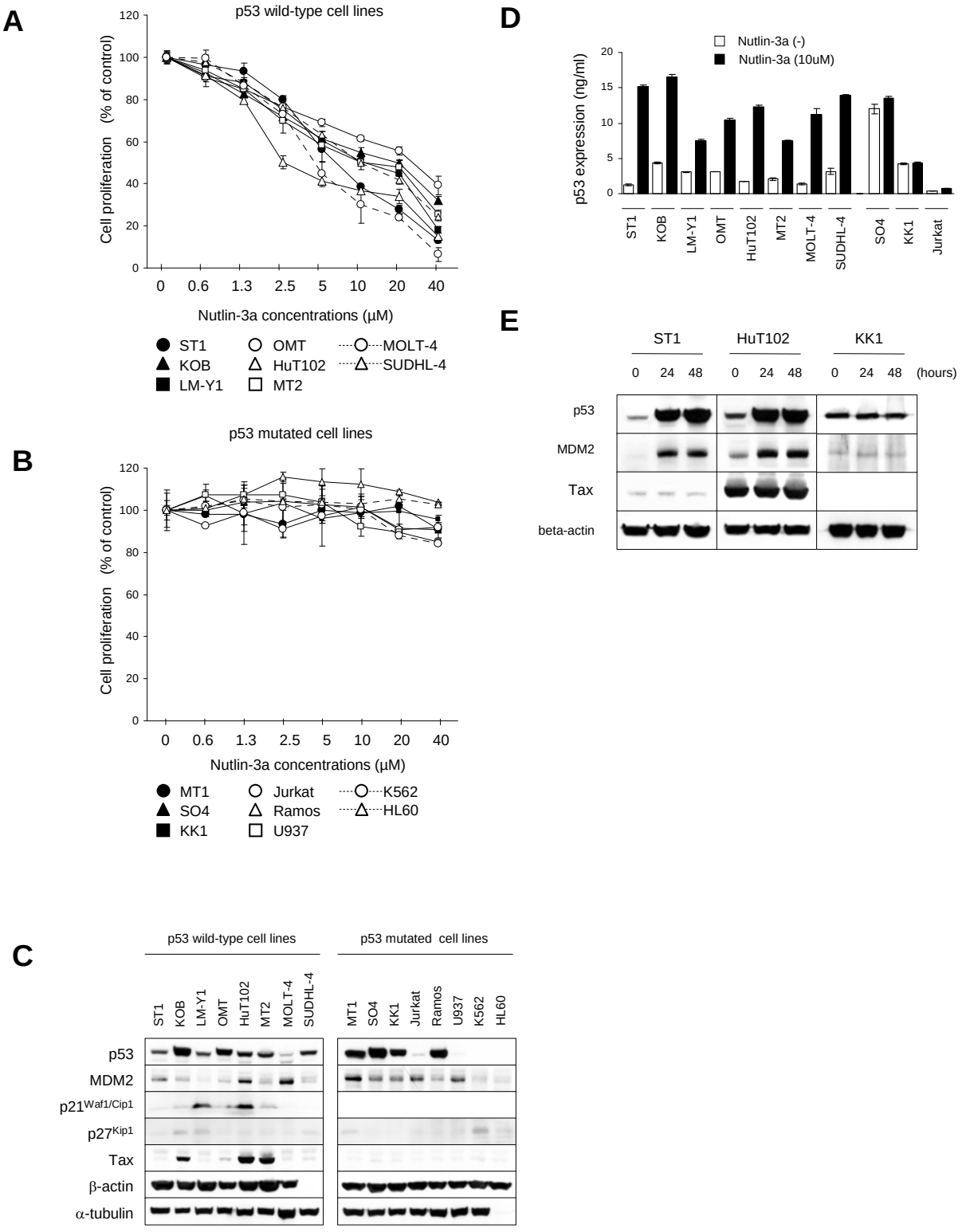
A
p53 wild-type cell lines
Cell proliferation (% of control)
Nutlin-3a concentrations (μM)
ST1
KOB
LM-Y1
OMT
HuT102
MT2
MOLT-4
SUDHL-4
B
p53 mutated cell lines
Cell proliferation (% of control)
Nutlin-3a concentrations (μM)
MT1
SO4
KK1
Jurkat
Ramos
U937
K562
HL60
C
p53 wild-type cell lines
p53 mutated cell lines
p53
MDM2
p21Waf1/Cip1
p27Kip1
Tax
β-actin
α-tubulin
D
Nutlin-3a (-)
Nutlin-3a (10uM)
p53 expression (ng/ml)
E
ST1
HuT102
KK1
(hours)
p53
MDM2
Tax
beta-actin

Figure 2

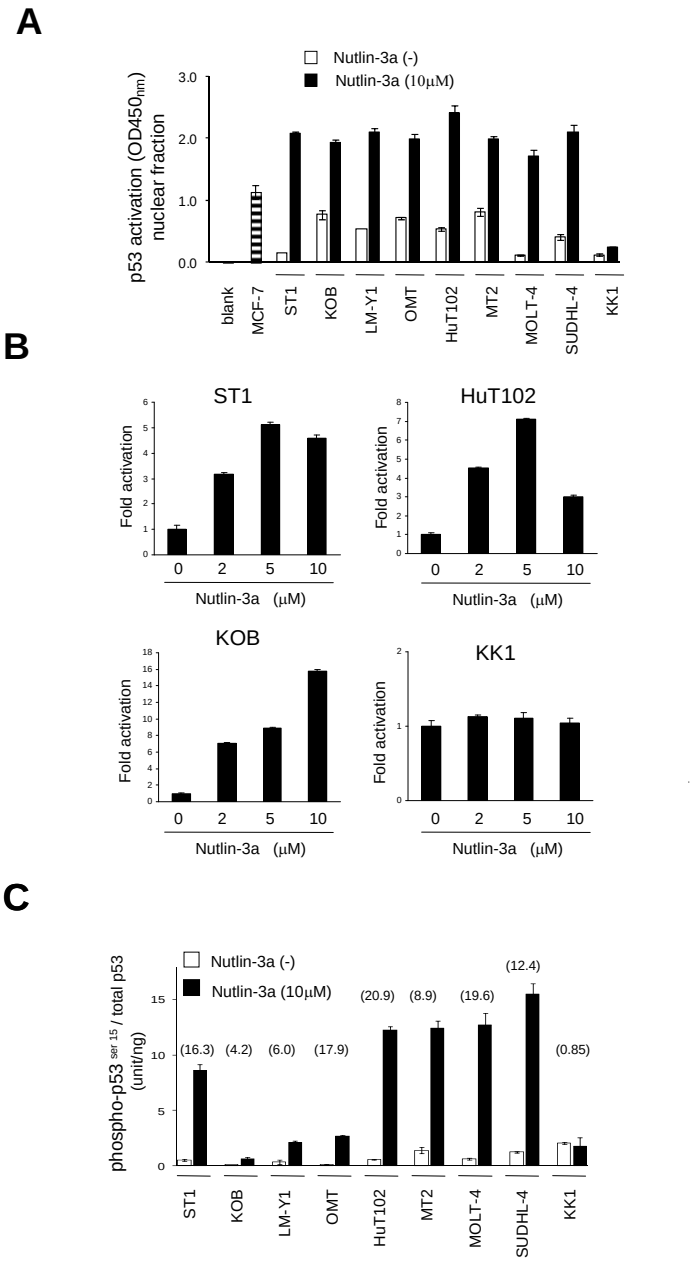
A
Nutlin-3a (-)
Nutlin-3a (10μM)
p53 activation (OD450nm)
nuclear fraction
3.0
2.0
1.0
0.0
blank
MCF-7
ST1
KOB
LM-Y1
OMT
HuT102
MT2
MOLT-4
SUDHL-4
KK1
B
ST1
HuT102
KOB
KK1
Fold activation
0
2
5
10
Nutlin-3a (μM)
C
Nutlin-3a (-)
Nutlin-3a (10μM)
phospho-p53 ser 15 / total p53
(unit/ng)
(16.3)
(4.2)
(6.0)
(17.9)
(20.9)
(8.9)
(19.6)
(12.4)
(0.85)
ST1
KOB
LM-Y1
OMT
HuT102
MT2
MOLT-4
SUDHL-4
KK1

Figure 3

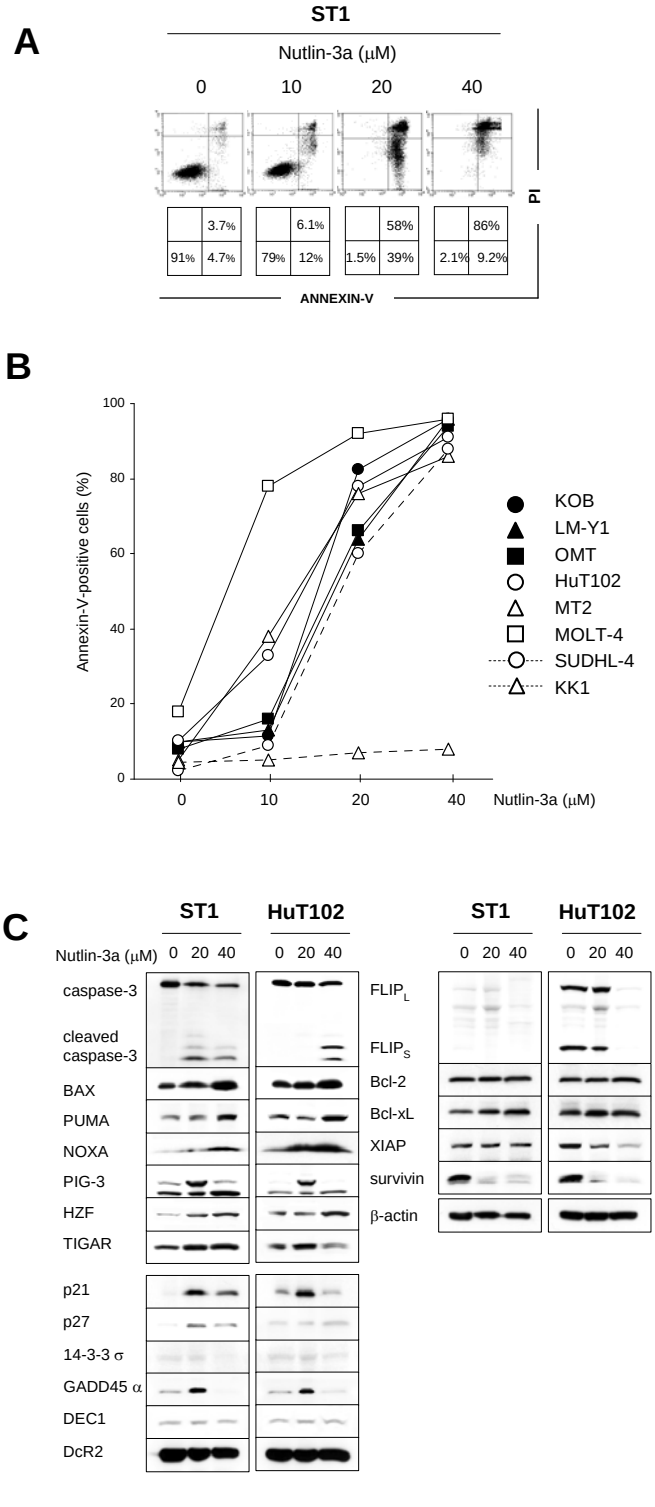
A
ST1
Nutlin-3a (μM)
0
10
20
40
3.7%
91%
4.7%
6.1%
79%
12%
58%
1.5%
39%
86%
2.1%
9.2%
PI
ANNEXIN-V
B
Annexin-V-positive cells (%)
100
80
60
40
20
0
0
10
20
40
Nutlin-3a (μM)
KOB
LM-Y1
OMT
HuT102
MT2
MOLT-4
SUDHL-4
KK1
C
ST1
HuT102
ST1
HuT102
Nutlin-3a (μM) 0 20 40
0 20 40
0 20 40
0 20 40
caspase-3
cleaved caspase-3
BAX
PUMA
NOXA
PIG-3
HZF
TIGAR
p21
p27
14-3-3 σ
GADD45 α
DEC1
DcR2
FLIP$_L$
FLIP$_S$
Bcl-2
Bcl-xL
XIAP
survivin
β-actin

Figure 4

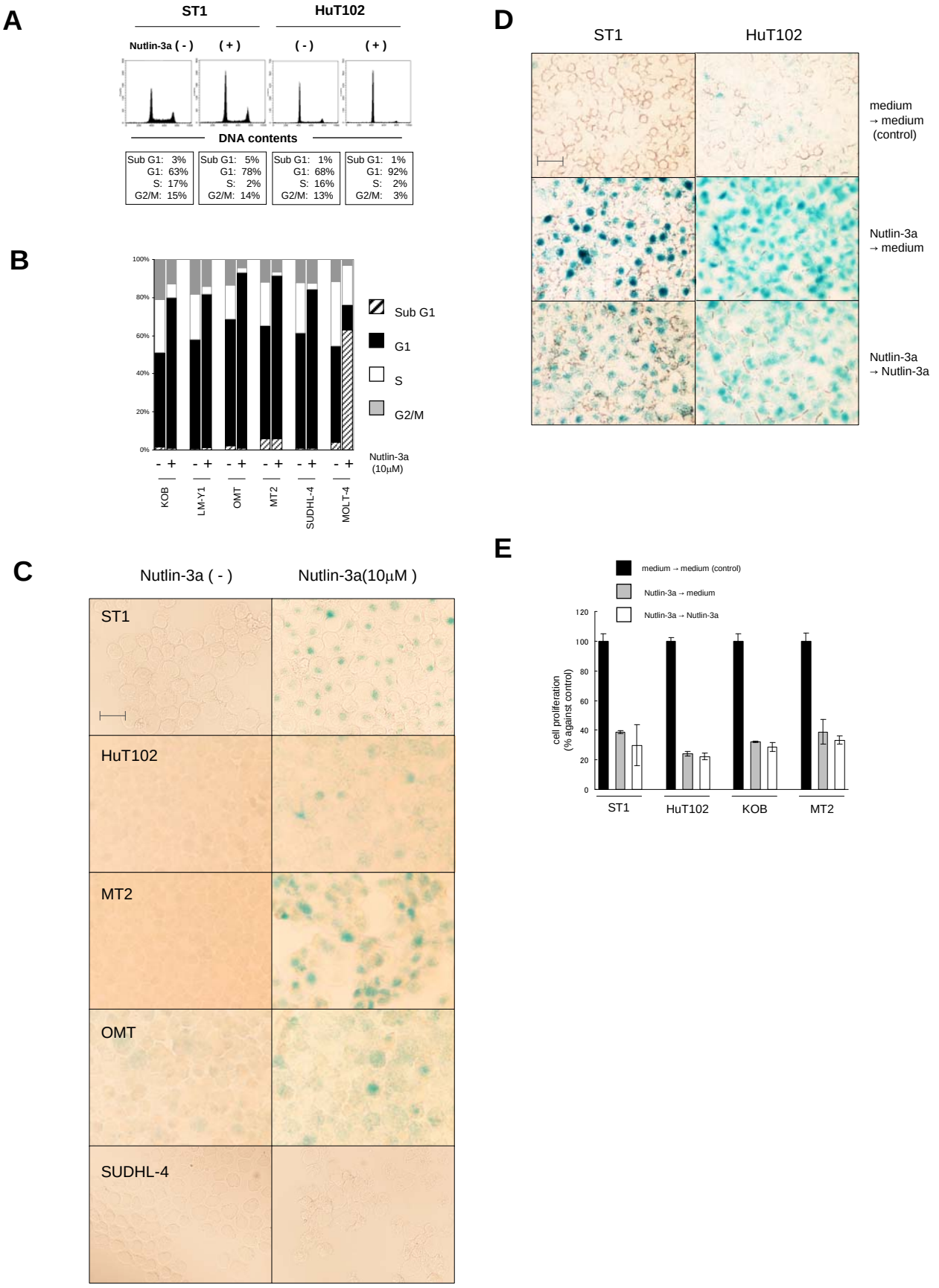
A
ST1
HuT102
Nutlin-3a (-)
(+)
(-)
(+)
DNA contents
Sub G1: 3%
G1: 63%
S: 17%
G2/M: 15%
Sub G1: 5%
G1: 78%
S: 2%
G2/M: 14%
Sub G1: 1%
G1: 68%
S: 16%
G2/M: 13%
Sub G1: 1%
G1: 92%
S: 2%
G2/M: 3%
B
100%
80%
60%
40%
20%
0%
Sub G1
G1
S
G2/M
Nutlin-3a (10μM)
KOB
LM-Y1
OMT
MT2
SUDHL-4
MOLT-4
C
Nutlin-3a (-)
Nutlin-3a(10μM)
ST1
HuT102
MT2
OMT
SUDHL-4
D
ST1
HuT102
medium → medium (control)
Nutlin-3a → medium
Nutlin-3a → Nutlin-3a
E
medium → medium (control)
Nutlin-3a → medium
Nutlin-3a → Nutlin-3a
cell proliferation (% against control)
120
100
80
60
40
20
0
ST1
HuT102
KOB
MT2

Figure 5

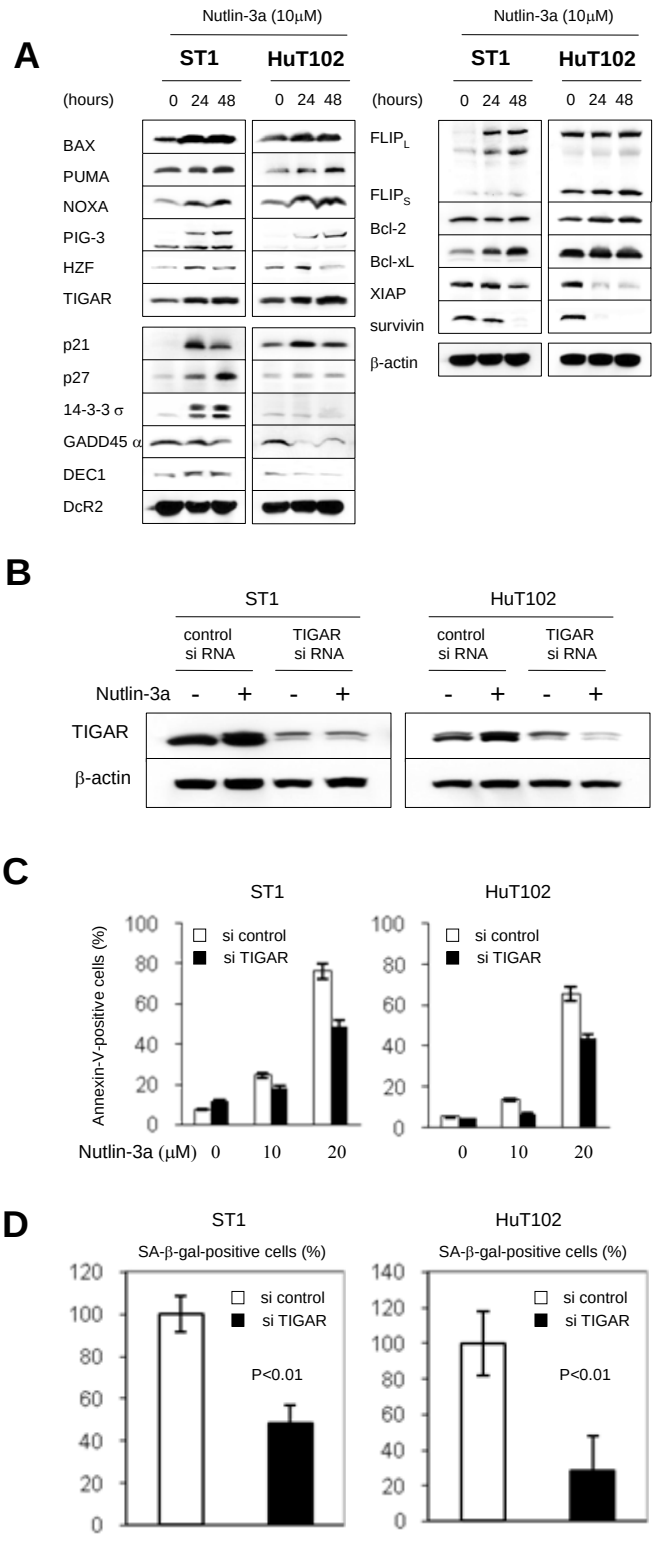
A
Nutlin-3a (10μM)
ST1
HuT102
(hours)
0 24 48
BAX
PUMA
NOXA
PIG-3
HZF
TIGAR
p21
p27
14-3-3 σ
GADD45 α
DEC1
DcR2
FLIP$_L$
FLIP$_S$
Bcl-2
Bcl-xL
XIAP
survivin
β-actin
B
ST1
HuT102
control si RNA
TIGAR si RNA
Nutlin-3a - + - +
TIGAR
β-actin
C
ST1
HuT102
Annexin-V-positive cells (%)
si control
si TIGAR
Nutlin-3a (μM) 0 10 20
D
ST1
HuT102
SA-β-gal-positive cells (%)
si control
si TIGAR
P<0.01

Figure 6

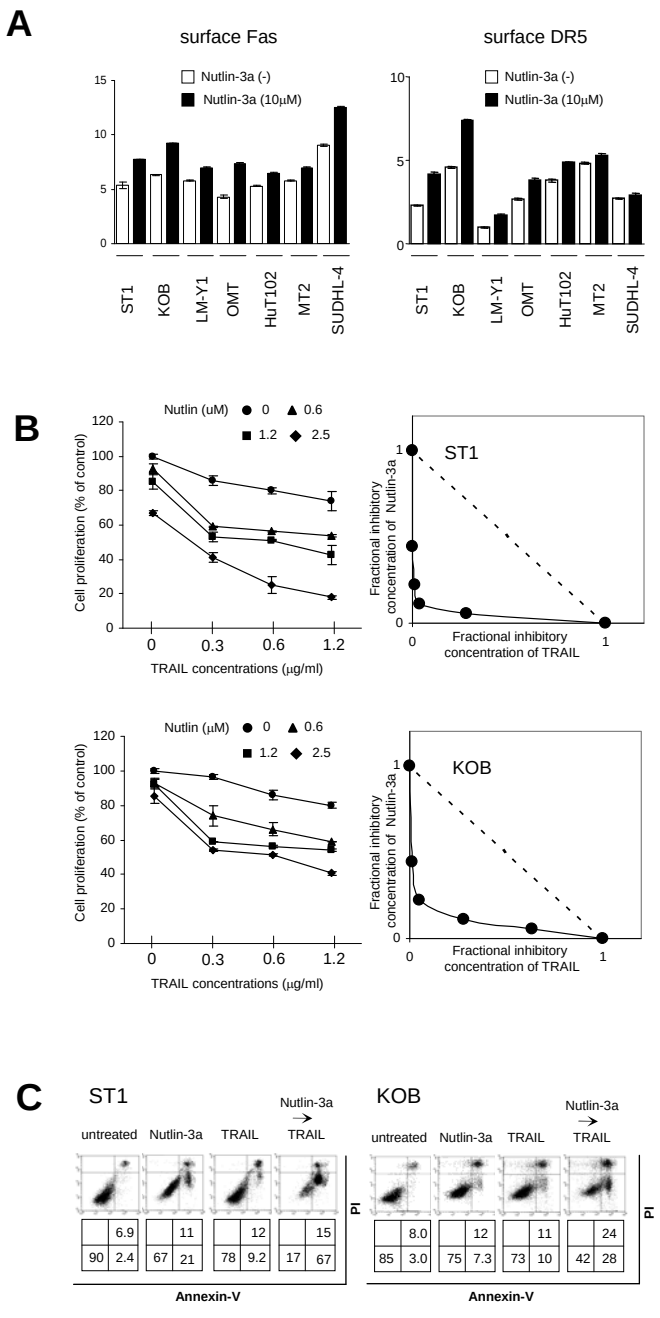
A
surface Fas
surface DR5
Nutlin-3a (-)
Nutlin-3a (10μM)
ST1
KOB
LM-Y1
OMT
HuT102
MT2
SUDHL-4
B
Nutlin (uM) 0 0.6 1.2 2.5
Cell proliferation (% of control)
TRAIL concentrations (μg/ml)
Fractional inhibitory concentration of Nutlin-3a
Fractional inhibitory concentration of TRAIL
ST1
Nutlin (μM) 0 0.6 1.2 2.5
KOB
C
ST1
KOB
untreated
Nutlin-3a
TRAIL
Nutlin-3a → TRAIL
PI
Annexin-V
6.9
90
2.4
11
67
21
12
78
9.2
15
17
67
8.0
85
3.0
12
75
7.3
11
73
10
24
42
28

Table 1. Mutations of p53 and deletions of *p14* and/or *p16*. p53 status was determined by direct sequence targeting of the open reading frame, following RNA isolation, cDNA synthesis and RT-PCR amplification (GenBank Accession number NM_000546). Deletions of *p14* and *p16* were determined using genomic DNA by the real-time quantitative PCR method based on TaqMan chemistry (GenBank Accession number AF527803). Quantitative analysis of HTLV-1 Tax mRNA expression was also performed. SNP: single nucleotide polymorphism; WT: wild type; MUT: mutation; del: deletion; ins: insertion; blank column: intact; N.D.: not determined.

Table 1

cell line	origin	exon	codon number	WT codon	Mutant codon	effect	p53 status	*p16*^{INK4a} / *p14*^{ARF}	HTLV-1 Tax mRNA
ST1	ATL	4	72	CCC	CGC	missence (SNP)	**WT**	del / del	0.4
KOB	ATL	4	72	CCC	CGC	missence (SNP)	**WT**	del / del	542
LM-Y1	ATL	4	36	CCG	CCA	silent	**WT**	del / del	1741
MT1	ATL	5	149	TCC	TTC	missence	**MUT**	del / del	17.5
KK1	ATL	3	31	GTT	ATT	missence	**MUT**	del / del	0.3
		5	152	CCG	CTG	missence			
SO4	ATL	6	223	CCT	CAT	missence	**MUT**	del / del	0.2
OMT	HTLV-I infected T-cell	4	72	CCC	CGC	missence (SNP)	**WT**	del / del	971
HuT102	HTLV-I infected T-cell						**WT**		2381
MT2	HTLV-I infected T-cell						**WT**		9331
MOLT-4	T-cell leukemia						**WT**	del / del	N.D.
Jurkat	T-cell leukemia	4	125	ACG	ACA	silent	**MUT**	del / del	0
		6	196	CGA	TGA	nonsence			
SUDHL-4	B-cell lymphoma						**WT**	del /	N.D.
Ramos	B-cell lymphoma	7	254	ATC	GAC	missence	**MUT**		N.D.
U937	Monocytic leukemia	4	105	GGC	AGC	missence	**MUT**	del / del	N.D.
		4	125	ACG	ACA	silent			
		6	196	CGA	TGA	nonsence			
K562	Erythroblastic leukemia	5	136			ins 1	**MUT**	del / del	N.D.
HL60	Myeloid leukemia			gross deletion			**MUT(deletion)**		N.D.